Recent advancements in Global-Local analysis of UGW in plates

Antonino Spada[1][0000−0002−5776−9940], Francesco Lanza di Scalea[2], Daniele Giardina[1], and Margherita Capriotti[3][0000−0002−6210−2657]

[1] Department of Engineering, University of Palermo, Viale delle Scienze, Ed. 8, 90128, Palermo, Italy. antonino.spada@unipa.it
[2] Experimental Mechanics NDE Laboratory, Department of Structural Engineering, University of California San Diego, 9500 Gilman Drive, La Jolla, CA 92093-0085, USA
[3] Aerospace Engineering Department, San Diego State University, 5500 Campanile Dr., 92182, San Diego, CA

Abstract. The use of ultrasonic guided waves (UGWs) has increased considerably for NDE and SHM purposes. Analytical solutions are available for few cases only, namely for waveguides of uniform cross-section and in the presence of simple defects. For more complex structural configurations, materials or defects, numerical methods are indispensable. A good compromise is coupling analytical solutions with numerical methods, as in the proposed hybrid Global-Local (GL) method. An eigenvalue problem in the framework of the Semi Analytical Finite Element method (SAFE) is posed to solve for the complex wavenumber and wavemodes, that are then propagated analytically in the wave propagation direction. To include scattering and wave propagation from the UGW interaction with geometrical dis-continuities, damages, and any changes along the wave propagation direction, SAFE is coupled with other computational approaches such as full FEM in this work. The complexity of UGW scattering is increased by the presence of propagating and non-propagating modes, the latter becoming significant in the near-field effects, i.e. in the vicinity of defect edges. This work shows the advantages of including the evanescent modes in the accurate modeling of UGWs scattering through applications on isotropic aluminum plates.

Keywords: Evanescent modes · Scattering · Defect · Ultrasonic Guided Waves · Structural Health Monitoring.

1 Introduction

The use of ultrasonic guided waves (UGWs) has increased considerably for NDE and SHM purposes, in a variety of materials, geometries and applications.

Analytical solutions are available for waveguides of uniform cross-section only or in cases where discontinuities or defects are easily defined by boundary conditions [1]. For complex geometries, materials or defects, computationally expensive numerical methods are required ([1]-[2]).

In order to drastically reduce the computational effort, hybrid methods have been proposed, by coupling analytical and numerical solutions. Mal and Chang [3] first proposed a hybrid method to calculate the elastodynamic field in a plate containing geometric discontinuities. The most diffused one is the Global-Local (GL) method ([4]-[7]), which couples the Semi Analytical Finite Elements method (SAFE) ([8]-[10]) with a full finite element discretization of the waveguide. SAFE method is applied on waveguide segments having non-variant and sound cross-section with even arbitrary geometry and varying material properties. The cross-section is discretized with FE and an eigenvalue problem is then posed to solve for the complex wavenumber and wavemodes, that are then propagated analytically, in the wave propagation direction. On waveguide segments containing geometrical discontinuities or defects, instead, a classical finite element analysis in all directions is performed. In these zones, indeed, because of scatterings from the anomalies, analytical solutions are no longer available.

The accuracy of the hybrid method is influenced by some parameters and is assessed through an energy balance. Displacements in each cross-section are evaluated as a combination of a fixed number of structural modes. Consequently, the total energy carried by the guided wave is numerically evaluated as the sum of the energies of the modes included into the analysis. Also, since the least-squares method is applied to evaluate the amplifiers of the combination, greater is the order of the governing matrix more correct will be the result.

A second aspect regards the numerical discretization. Known discretization rules have to be applied to relate the element size to the wavelength. It is therefore important to pay attention to the element size, according to the frequency range of interest.

A third aspect regards the presence of propagating and also non-propagating modes. This aspect is of particular importance when the contribution of near-field effects cannot be neglected, such as in the vicinity of defect edges. [11] studied the effect of propagating and non-propagating modes concluding that different solution methods require a different number of modes to satisfy energy balance. [8] studied UGWs propagation in damped and undamped waveguides of isotropic and composite materials with the SAFE method, including evanescent modes. [12] and [13] used the modal decomposition method. They concluded that, although the power flow has to be computed only for incident and scattered propagative modes, the energy balance must include complex (evanescent) modes to satisfy boundary conditions, hence to obtain an accurate solution. The CMEP method was more recently used by [1] in 2D aluminum plates with horizontal cracks: a convergence analysis was performed to assess the number of complex roots to be included. [14] studied the scattering from horizontal cracks in an aluminum plate, using the Wave FE method. [15] validated the hybrid method studying UGWs scattering in cylindrical waveguides: the number of non-propagating modes to be included in the analysis for an accurate result was decided depending on the magnitude of the imaginary part of the product wavenumber and radius.

In this paper, the authors investigate the role of evanescent modes in the accurate modeling of UGWs scattering in 2 mm isotropic aluminum plates. An answer is given to the question on which is the minimum distance between the scatterer and the boundary of the full FE segment, in order to obtain an accurate solution when evanescent modes are not included in the analysis.

2 Theoretical formulation

The GL method formulates the UGW propagation problem by identifying two regions in the complex waveguide (Fig. 1): the local region, containing the defect, and the global region, representing an infinite waveguide of arbitrary cross-section. The formulation is here briefly summarized in 2D. A detailed formulation can be found in [4]. An incident time-harmonic guided wave excited in the sound (global) region propagates along the wave propagation direction and is scattered into reflected and transmitted waves, after interacting with the discontinuity within the local region. The equilibrium of each region is guaranteed by imposing the Principle of Virtual Work (PVW).

The cross-section in the global region is discretized by FE, while the harmonic exponential term $e^{i(\xi x-\omega t)}$ describes the analytical wave propagation. ξ is the wavenumber and ω the angular frequency. The stiffness matrix $\mathbf{K}^g$, mass matrix $\mathbf{M}^g$ and force vector $\mathbf{F}^g$ are computed for the global region and the PVW is applied, obtaining:

$$(\mathbf{K}^g - \omega^2\mathbf{M}^g)\mathbf{U}^g = \mathbf{F}^g. \tag{1}$$

The right-side of Eq. (1) is 0 in the case of an unforced solution. This reduces to an eigenvalue problem, where the wavenumbers ξ and wavemodes ϕ can be found in terms of eigenvalues and eigenvectors. The eigenvalues can be pairs of real, complex and imaginary numbers, representing propagating, evanescent decaying and evanescent non-oscillating (end-modes) waves, respectively.

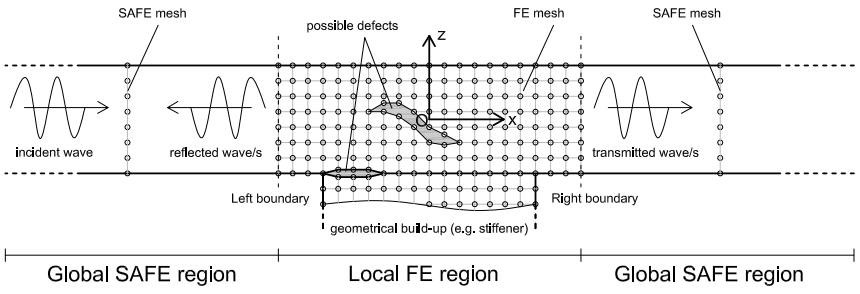

Fig. 1: Scattering of an incident wave into reflected and transmitted modes.

Following [15], a threshold equal to $Im(\xi h) = [-5, 5]$ has been placed to select the evanescent modes, where h is the thickness of the waveguide. Phase and group velocity are then computed as $c_p = \omega/\xi_{Re}$ and $c_g = \frac{\partial\omega}{\partial\xi}$, as well as attenuation $att = \xi_{Im}$ and energy velocity $c_{En} = \frac{\frac{1}{T}\int_\Gamma \boldsymbol{P}\cdot\boldsymbol{n}d\Gamma}{\frac{1}{T}\int_T(\frac{1}{\Gamma}\int_\Gamma e_{tot}d\Gamma)dt}$, where Γ is the cross-sectional area, $\boldsymbol{P}$ is the Poynting vector (real part only), $\boldsymbol{n}$ is the propagation direction unit vector, e_{tot} is the total energy density (kinetic and potential), T is the period.

The nodal displacements at the left boundary $\boldsymbol{q}_{lB}$ of the local region are the combination of the incident wave and the reflected waves, while those at the right boundary $\boldsymbol{q}_{rB}$ are a combination of the transmitted waves only.

In the case of UGW propagation and scattering, the incident, reflected and transmitted waves can be thought of as the superposition of weighted N_M wave-modes, corresponding to the global cross-sectional modeshapes obtained in the SAFE solution. Therefore:

$$\boldsymbol{q}_{lB} = \boldsymbol{\Phi}^{+}_{in} e^{i[\xi^{+}_{in}(x_S - x_{lB})]} + \sum_{j=1}^{N_M} A^{-}_{j} \boldsymbol{\Phi}^{(j)^{-}} e^{i(\xi^{-}_{j} x_{lB})}; \tag{2}$$

$$\boldsymbol{q}_{rB} = \sum_{j=1}^{N_M} A^{+}_{j} \boldsymbol{\Phi}^{(j)^{+}} e^{i(\xi^{+}_{j} x_{rB})}. \tag{3}$$

The weights are the amplitude A_j of the modeshapes, which are calculated by least square method on the system:

$$\boldsymbol{S}\,\boldsymbol{U}^l = \boldsymbol{F}^l \tag{4}$$

where $\boldsymbol{S}$ is the dynamic stiffness matrix for the local region, $\boldsymbol{U}^l$ and $\boldsymbol{F}^l$ the vectors containing the nodal displacements and forces at the local region, respectively. Such weights represent the scattering coefficients.

The energy carried by each j-th mode is calculated as:

$$E^j = -\frac{|A_j|^2}{2} Re[i\omega \boldsymbol{F}^{j\,T} \bar{\boldsymbol{\Phi}}^j]. \tag{5}$$

The total energy is the sum of the energy of all reflected $E^{(j)}_{Refl}$ and transmitted $E^{(j)}_{Transm}$ modes, given an incident energy E_{in} amplitude equal to 1,

$$E_{in} = \sum_{j=1}^{N_M} (E^{(j)}_{Refl} + E^{(j)}_{Transm}). \tag{6}$$

As stated in [12], evanescent modes do not carry energy. Their contribution is important for obtaining an accurate scattering solution, since boundary conditions are better satisfied.

3 Numerical investigations

The numerical analyses reported in this section were obtained by employing the Global-Local Matlab© code developed by [4], enhanced by adding the contribution of evanescent modes.

The importance of including the evanescent modes is here demonstrated through two simple applications on an aluminum plate having thickness equal to 2 mm. For both applications, the local zone has a length of 5 mm, while two types of defects are considered, namely a centered square defect and a centered rectangular notch on the top, as shown in Fig. (2). Different values of the parameter d defining the defect size are considered in each case. The analyzed frequency range is DC-1 MHz, with a frequency increment of 2 kHz and a total of 500 frequency steps. The FE mesh in the local zone is composed by linear square elements with sides equal to 0.1 mm, in order to guarantee the common rule of at least 20 elements for wavelength in the direction of propagation.

Fig. (3) shows the dispersion curves obtained from the SAFE method applied to the global region. A total of 5 propagative modes and 6 evanescent modes are present in the analyzed frequency range. Solutions with evanescent modes include all 6 evanescent modes in addition to the 5 propagative modes.

Figs. (4) and (5) report the total energies obtained for the two analyzed cases, at varying d parameter. The inclusion of evanescent modes reflects in a better evaluation of the unknown coefficients, leading to a more accurate estimation of the energy and thereby reducing the error in energy conservation.

The accuracy of the numerical results is estimated as better as more the conservation of energy is respected, then when the total energy, normalized with respect to the incoming energy, is close to 1.

For the case of a centered square defect (Fig. 4), 5 total analyses were run, considering four different defects with increasing size (from 0.4 mm to 1.6 mm) other than the pristine conditions. In pristine conditions the conservation of energy is fully respected, demonstrating the goodness of the code in respecting the limit cases. When the defect increases in size, in absence of evanescent modes and for an A0 incoming mode (Fig. 4a), the normalized energy reduces drastically for certain frequencies, especially between 500 kHz and 800 kHz. Even with a square defect with size equal to 0.4 mm (local zone boundary - defect distance equal to 2.3 mm) the maximum error is 17% at 760 kHz. These errors are almost vanished in all defected conditions when evanescent modes are included (Fig. 4b).

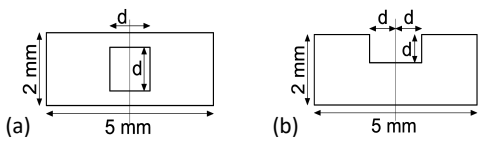

Fig. 2: Local zone of analyzed cases.

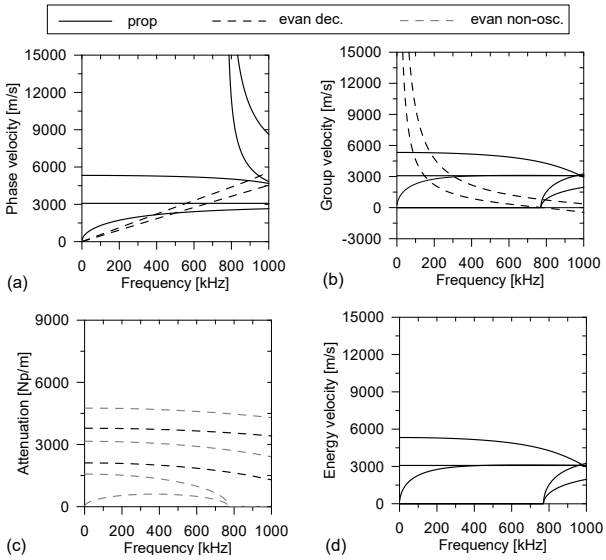

Fig. 3: 2 mm thick aluminum plate dispersion and attenuation curves: a) phase velocity, b) group velocity, c) attenuation, d) energy velocity.

When the S0 mode is incoming in absence of evanescent modes (Fig. 4c), the defect constitutes a more or less greater barrier to the wave. The solution is acceptable for a defect size of 0.4 mm and the maximum error is maximum 8% at 860 kHz. When $d = 1.2mm$ or $d = 1.6mm$ (local zone boundary - defect distance less than 2 mm) higher values of the error are reached, but for fixed frequencies only. The presence of evanescent modes in this case improves the solution, but still localized high error are present (Fig. 4d).

For the case of a centered rectangular notch (Fig. 5), 6 total analyses were run, considering five different defects with increasing size other than the pristine conditions. The base to height ratio is maintained equal to 2 (heights ranging from 0.2 mm to 1.0 mm). In pristine conditions the conservation of energy is again fully respected. In the presence of the defect, in absence of evanescent modes and for an A0 incoming mode (Fig. 5a), the scattering spectra have similar trends, with increasing errors as the notch increases in size. Till $d = 0.4mm$ (local zone boundary - defect distance more than 2 mm) the maximum error is of 5%. When evanescent modes are included, apart for d equal to 0.8 and 1 mm, the error is nullified (Fig. 5b). When the S0 mode is incoming, in the absence of evanescent modes (Fig. 5c), the trends of the total energies are again similar, with an increasing error at increasing d. The error does not overcome 10% till $d = 0.6mm$, arrives to a maximum of 13% with higher d values. With evanescent modes in the analyses, the error vanishes till the cut-on of higher order modes, but keeps below 5% (Fig. 5d).

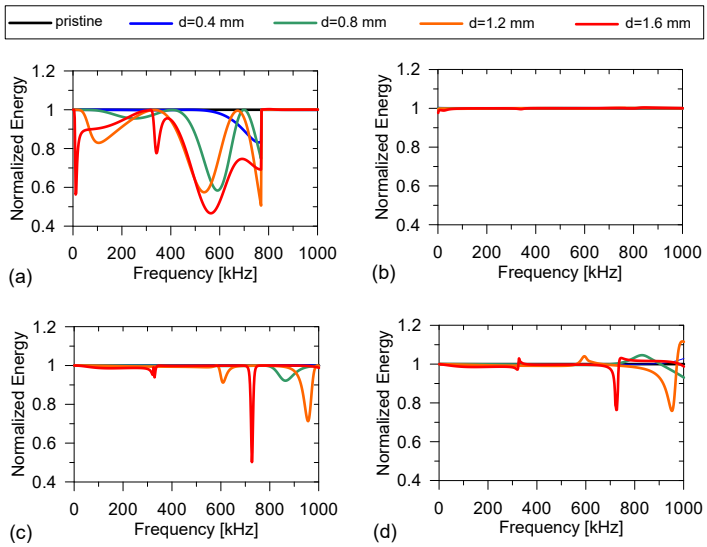

Fig. 4: Total energies for a square defect. (a, b) A0 incoming; (c, d) S0 incoming; (a, c) evanescent modes not included; (b, d) evanescent modes included.

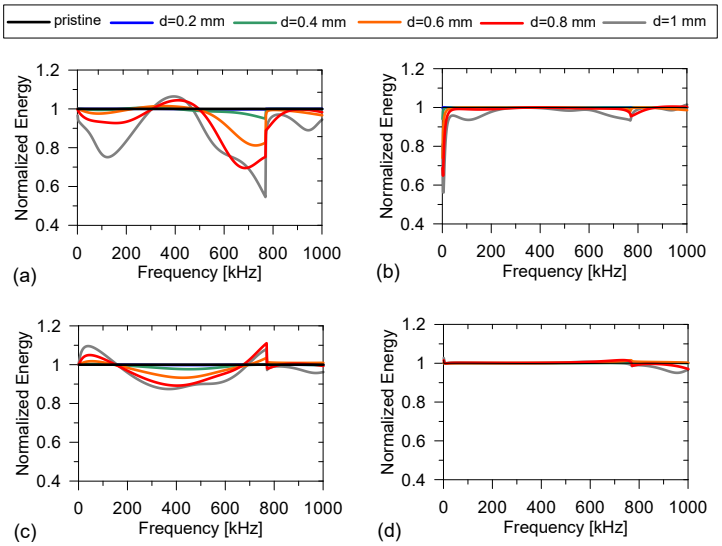

Fig. 5: Total energies for a rectangular notch. (a, b) A0 incoming; (c, d) S0 incoming; (a, c) evanescent modes not included; (b, d) evanescent modes included.

4 Concluding remarks.

In this paper the role of evanescent modes in Global-Local analysis of UGW in 2 mm aluminum plates with a centered square defect and a rectangular notch was investigated. The most important outcome of analyses is that, in the absence of evanescent modes, the minimum local zone boundary/defect distance should be at least equal to the plate thickness in order to have reduced errors (less than 10%). When evanescent modes are included the distance can be reduced till 1.5 the plate thickness. If the attention is not too much payed to localized errors, all analyses can be considered acceptable if evanescent modes are included.

Concluding, the absence of evanescent modes has two implications: it is necessary to always ensure a minimum local zone boundary/defect distance; error in the conservation of energy increases as the number of neglected evanescent modes increases. The presence of evanescent modes, on the other hand, has two benefits: it improves the Global-Local numerical solution, and it reduces to a minimum the length of the local zone, reducing computational costs, as well.

5 Acknowledgements

The first and third authors acknowledge the financial support for this research within the PRIN project 2022P7PF8J LASTEB.

References

1. Poddar, B., Giurgiutiu, V. Wave Motion, **65**, 79–91 (2016).
2. Willberg, C., Duczek, S., Vivar-Perez, J.M., Ahmad, Z.B. Appl. Mech. Reviews, **67**(1), (2025).
3. Mal, A., Chang. Z. Geophysical Journal International, **143**(2), 328–334 (2000).
4. Spada, A., Capriotti, M., Lanza di Scalea, F. Int J Solids Struct, **182**, 267–280 (2020).
5. Spada, A., Capriotti, M., Lanza di Scalea, F. Struct Health Monit, **21**(2), 370–386 (2022).
6. Srivastava, A., Lanza di Scalea, F. J Eng Mech, **136**(8), 937–944 (2010).
7. Spada, A., Zhang, M., Lanza di Scalea, F., Capriotti, M. JVC/Journal of Vibration and Control, article in press, doi: 10.1177/10775463231168926. (2023).
8. Bartoli, I., Marzani, A., di Scalea, F.L., Viola, E. JSV, **295**(3–5), 685–707 (2006).
9. Hayashi, T., Song, W.J., Rose, J.L. Ultrasonics, **41**(3), 175–183 (2003).
10. Marzani, A., Viola, E., Bartoli, I., Di Scalea, F.L., Rizzo, P. Journal of Sound and Vibration, **318**(3), 488-505 (2008).
11. Taweel, H., Dong, S.B., Kazic, M. Int. J. Solids Struct., **32**(12), 1701-1726 (2000).
12. Castaings, M., Le Clezio, E., Hosten, B. The Journal of the Acoustical Society of America, **112**(6), 2567-2582 (2002).
13. Diligent, O., Lowe, M.J.S., Le Clézio, E., Castaings, M., Hosten, B. The Journal of the Acoustical Society of America, **113**(6), 3032-3042 (2003).
14. Schaal, C., Zhang, S., Samajder, H., Mal, A. Proceedings of the Institution of Mechanical Engineers, Part C: J Mech Engrg Science, **231**(16), 2947-2960 (2017).
15. Benmeddour, F., Treyssède, F., Laguerre, L. Int J Solids Struct, **48**(5), 764-774 (2011).